DOI: 10.1002/ejic.200800196

Synthesis, Structural, Thermal and Magnetic Characterization of a Pyrophosphato-Bridged Cobalt(II) Complex

Oluwatayo F. Ikotun,[a] Wayne Ouellette,[a] Francesc Lloret,[b] Paul E. Kruger,[c] Miguel Julve,*[b] and Robert P. Doyle*[a]

Keywords: Cobalt complexes / Pyrophosphate / Magnetic coupling / Crystal structure / Polynuclear compounds

The reaction in water of Co^{II} sulfate heptahydrate with 1,10-phenanthroline (phen) and sodium pyrophosphate ($Na_4P_2O_7$) in a 2:4:1 stoichiometric ratio resulted in the crystallization of a neutral dinuclear Co^{II} complex, $\{[Co(phen)_2]_2(\mu\text{-}P_2O_7)\}\cdot 6MeOH$ (**1**), as revealed by a single-crystal X-ray diffraction study. The bridging pyrophosphato ligand between the two $[Co(phen)_2]^{2+}$ units in a bis(bidentate) coordination mode places the adjacent metal centers at 4.857 Å distance, and its conformation gives rise to intramolecular π–π stacking interaction between adjacent phen ligands. Indeed, intermolecular π–π stacking interactions between phen ligands from adjacent dinuclear complexes create a supramolecular 2D network in **1**. Magnetic susceptibility measurements on a polycrystalline sample of **1** in the temperature range 1.9–295 K are typical of an overall antiferromagnetic coupling with a maximum of the magnetic susceptibility at 3.0 K. The analysis of the magnetic data in the whole temperature range allows the determination of the value of the intramolecular magnetic coupling ($J = -1.23\ cm^{-1}$). The ability of the pyrophosphato ligand to mediate magnetic interactions between different first-row transition-metal ions when adopting the bis(bidentate) bridging mode is analyzed and discussed in the light of the small number of magneto-structural reports on this type of compound, bearing in mind the number of unpaired electrons and type of magnetic orbitals on each metal center.

Introduction

Cobalt is an essential trace element found in the active sites of metalloenzymes such as the human methionine aminopeptidases (MetAP2),[1] and as the metal cofactor in vitamin B_{12}.[2] The pivotal role played by divalent metal ions such as Co^{II} in the cellular management of inorganic oxo anions such as phosphate and pyrophosphate (diphosphate) is exemplified by the inorganic pyrophosphatases (PPases).[3] PPases are cytoplasmic enzymes that hydrolyze pyrophosphate ($P_2O_7^{4-}$) to inorganic phosphate.[4] Divalent metal ions are required for activity in all PPases. The efficiency of these cations as activators decreases in the order $Mg^{II} > Zn^{II} > Co^{II} > Mn^{II} > Cd^{II}$.[5] These enzymes can have as many as four functional divalent metal ions at the active site: two metal ions are bound as essential cofactors, while the third and fourth are attached to pyrophosphate/phosphate forming substrate/product motifs.[6]

In addition to their biological functions, pyrophosphate salts have aroused interest as materials for laser hosts in ceramics, electric, catalytic and magnetic applications.[7] The ability of pyrophosphate to act as a complexing agent makes it potentially capable of mediating electronic interactions between paramagnetic metal centers. Despite the diversity and importance of pyrophosphate interactions with metal ions, there remains a scarcity of structurally characterized coordination complexes (Table 1),[8] most likely as a consequence of the pyrophosphate's hydrolytic sensitivity especially in the presence of divalent metal ions.[6]

Given the relevance of pyrophosphate in biological and materials science, we have focused our recent efforts on the synthesis of coordination complexes containing pyrophosphato ligands, aiming at establishing a correlation between the structural and magnetic properties of these species. In this report, we present the synthesis, structural characterization, magnetic investigation and thermal study of the first pyrophosphato-bridged Co^{II} coordination complex, and we discuss its place in the growing understanding of pyrophosphate's ability to mediate magnetic interactions between paramagnetic metal ions.

---

[a] Department of Chemistry, Syracuse University,
Syracuse, NY 13244-4100, USA
Fax: +1-315-443-4070
E-mail: rpdoyle@syr.edu
[b] Departament of Química Inorgànica/Instituto de Ciencia Molecular (ICMol), Universitat de Valencia,
Polígono la Coma s/n, 46980 Paterna (Valencia), Spain
E-mail: miguel.julve@uv.es
[c] Department of Chemistry, College of Science, University of Canterbury,
Christchurch 8020, New Zealand

Table 1. Structurally characterized polynuclear complexes featuring the bridging pyrophosphato ligand.[a]

Metal	Compound	Space group	Ref.
Cu^{II}	$[(CuL)_4(\mu\text{-}P_2O_7)]\cdot nH_2O$	$C2/c$	[9]
Cu^{II}	$\{[Cu(bipy)(H_2O)]_2(\mu\text{-}P_2O_7)\}\cdot 7H_2O$	$P\bar{1}$	[10]
Cu^{II}	$\{[Cu(bipy)(H_2O)(\mu\text{-}P_2O_7)Na_2(H_2O)_6]\}\cdot 4H_2O$	$P\bar{1}$	[3]
Cu^{II}	$\{[Cu_4(dpa)_4(\mu\text{-}P_2O_7)_2]\}\cdot 11H_2O$	$P2_1/n$	[11]
Co^{III}	$\{[Co(tpa)]_2(\mu\text{-}P_2O_7)\}(ClO_4)_2\cdot 2.5H_2O\cdot 2.5MeOH$	$P\bar{1}$	[12]
Co^{II}	$\{[Co(phen)_2]_2(\mu\text{-}P_2O_7)\}\cdot 6MeOH$	$P\bar{1}$	this work
Zn^{II}	$\{[Zn(bipy)(H_2O)(\mu\text{-}P_2O_7)Zn(bipy)]_2\}\cdot 14H_2O$	$P2_1/c$	[3]
$V^{II}O$	$(tmp)_4[(VO)_4(\mu\text{-}P_2O_7)_2(\mu\text{-}OMe)_4]$	$P2_1/n$	[13]
Ni^{II}	$\{[Ni(phen)_2]_2(\mu\text{-}P_2O_7)\}\cdot 27H_2O$	$I4_1/acd$	[8]
Mn^{II}	$\{[Mn(phen)_2]_2(\mu\text{-}P_2O_7)\}\cdot 13H_2O$	$P\bar{1}$	[8]

[a] Abbreviations: n = 9–12; bipy = 2,2′-bipyridine; dpa = 2,2′-dipyridylamine; L = 2-formylpyridine thiosemicarbazone; tpa = tris(2-pyridylmethyl)amine; tmp = 2,4,6-trimethylpyridine; phen = 1,10-phenanthroline.

Results and Discussion

Synthesis and Characterization of $\{[Co(phen)_2]_2(\mu\text{-}P_2O_7)\}\cdot 6MeOH$ (1)

An aqueous solution of cobalt(II) sulfate heptahydrate was treated with an aqueous suspension of 1,10-phenanthroline in a 1:2 molar ratio, resulting in the formation of a clear orange solution upon stirring. A peach-colored precipitate was formed upon addition of 0.5 equiv. of solid sodium pyrophosphate. This precipitate was re-dissolved in a minimal amount of methanol and red block crystals were obtained by vapor diffusion with petroleum ether into this solution over a period of 6 d. The IR spectrum of these crystals shows a broad band at 1103 cm^{-1} with shoulders at 1180 and 1021 cm^{-1}, which is indicative of pyrophosphate, and bands at 1516 and 1424 cm^{-1}, assigned to the presence of the phen ligands.[14] Electrospray mass spectrometry gave a peak at m/z = 507.1 with the correct isotopic distribution and m/z spacing for the desolvated parent species, $[Co_2(phen)_4(\mu\text{-}P_2O_7)]$ with z = 2.

Crystal Structure of 1

The atom numbering scheme and the atomic connectivity of **1** are shown in Figure 1. **1** crystallizes in the triclinic $P\bar{1}$ space group.

The dinuclear entity is made up of two crystallographically unique $[Co(phen)_2]^{2+}$ units bridged by the tetraanionic pyrophosphato ligand with six methanol molecules of crystallization throughout the lattice. Similar to previously published dinuclear Ni^{II} and Mn^{II} pyrophosphate complexes,[8] the pyrophosphato ligand coordinates to the metal center in a bis(bidentate) coordination mode forming two six-membered chelate rings. The geometry of the unique cobalt atoms [Co(1) and Co(2)] is distorted octahedral with four nitrogen atoms from two phen ligands and two pyrophosphate oxygen atoms providing each cobalt atom with an N_4O_2 donor set (N_2O_2 equatorial arrangement with axial nitrogen atoms). The best equatorial plane for Co(1) is defined by the N2,N3,O6,O7 set of atoms with a torsion angle of 16.68°, with the cobalt atom displaced by 0.004 Å from the mean plane. For Co(2) the best equatorial plane

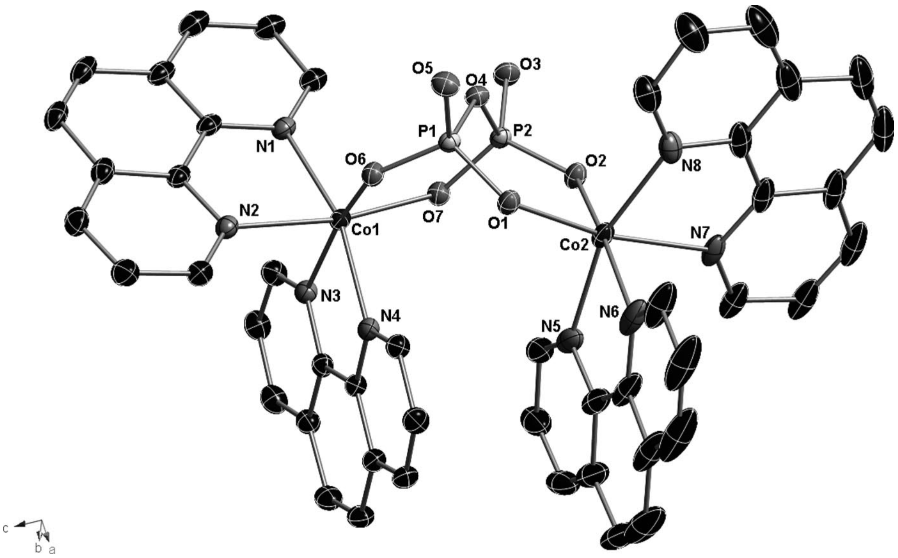

Figure 1. ORTEP plot (at 40% probability) of **1** with the atom labelling scheme; hydrogen atoms and methanol molecules of crystallization are omitted for clarity.

Table 2. Selected bond lengths [Å] and angles [°] for **1**.

Co(1)–O(6)	2.0283(12)	O(7)–Co(1)–N(3)	90.88(5)
Co(1)–O(7)	2.0525(12)	O(6)–Co(1)–N(2)	88.48(5)
Co(1)–N(1)	2.1353(14)	O(6)–Co(1)–O(7)	94.08(5)
Co(1)–N(2)	2.1750(15)	N(2)–Co(1)–N(3)	89.01(5)
Co(1)–N(3)	2.1936(14)	N(4)–Co(1)–N(3)	76.78(5)
Co(1)–N(4)	2.1312(14)	N(1)–Co(1)–N(2)	76.88(6)
Co(2)–O(1)	2.0760(12)	O(1)–Co(2)–N(5)	103.65(6)
Co(2)–O(2)	2.0148(12)	O(1)–Co(2)–N(8)	92.20(6)
Co(2)–N(5)	2.1519(18)	O(2)–Co(2)–O(1)	94.45(5)
Co(2)–N(6)	2.1663(17)	N(8)–Co(2)–N(7)	76.36(7)
Co(2)–N(7)	2.2066(16)	N(5)–Co(2)–N(7)	87.75(7)
Co(2)–N(8)	2.1593(18)	N(5)–Co(2)–N(6)	76.41(8)
P(1)–O(5)	1.5106(13)	O(1)–P(1)–O(6)	112.76(7)
P(1)–O(4)	1.6209(12)	O(2)–P(2)–O(7)	112.20(7)
P(2)–O(3)	1.5054(13)	P(1)–O(4)–P(2)	123.41(7)
P(1)–O(6)	1.516(12)	P(2)–O(4)	1.634(12)
P(2)–O(2)	1.518(12)	P(2)–O(7)	1.521(12)

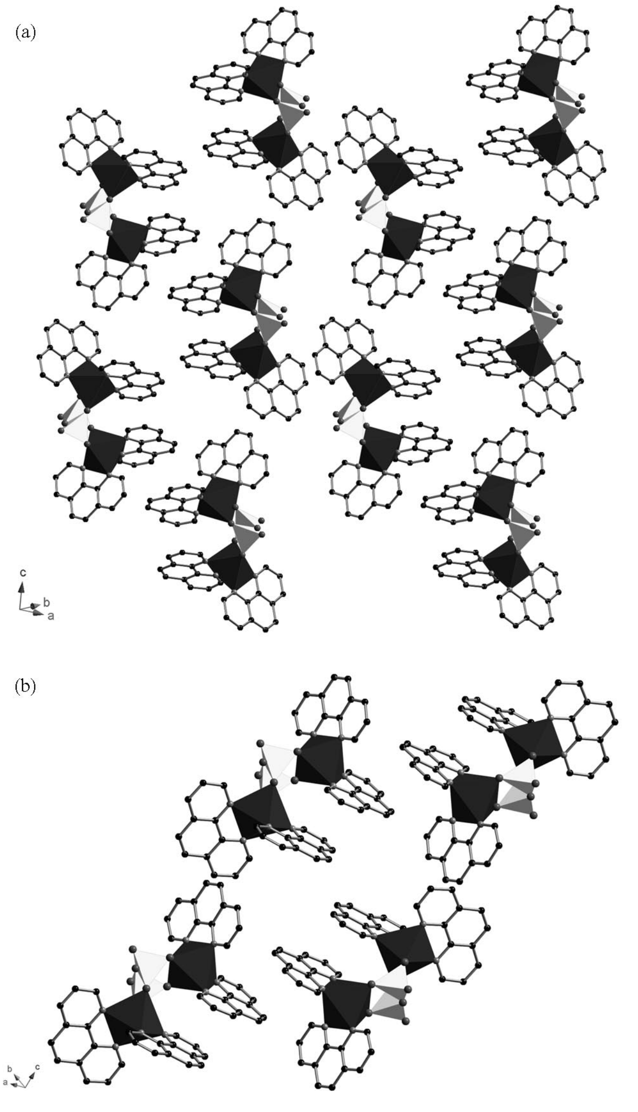

Figure 2.(a) Packing diagram of **1** viewed along the crystallographic *c*-axis. Note the intra- and intermolecular π–π interactions. Hydrogen atoms and lattice methanol molecules have been omitted for clarity. (b) Packing diagram of **1** showing the 1D sheet running along the crystallographic *c*-axis.

is described by the N6,N7,O1,O2 set with a torsion angle of 21.18° with the cobalt atom displaced by 0.019 Å from the mean plane. The angle between both cobalt equatorial planes is 28.01°.

The terminal P=O bonds in the bridging pyrophosphato ligand are shorter at 1.511 Å [P(1)–O(5)] and 1.505 Å [P(2)–O(3)] compared with the inner P–O bonds, whose lengths range between 1.516 Å [P(1)–O(6)] and 1.634 [P(2)–O(4)]. Selected bond lengths and angles are shown in Table 2.

The cobalt–cobalt distance across the pyrophosphato bridge is 4.857 Å, a value which lies in the range of those observed for other pyrophosphato-bridged dinuclear complexes with first-row transition-metal ions [4.646–5.031 Å].[8,10] The shortest interdimer Co···Co distance in **1** is 9.911 Å. The phen ligands about Co(1) and Co(2) interact with each other through intramolecular face-to-face π–π stacking with a separation at closest contact of 3.61 Å. Adjacent phen ligands also interact through intermolecular edge-to-face and face-to-face π–π interactions (Figure 2a). These interactions result in the formation of pseudo-layers with the lattice methanol molecules residing between the layers (see Figure 2b). The volume occupied by the solvent of crystallization is 26.1% which is significantly lower than that observed for previously reported structures (e.g. the Ni^{II} complex has the highest solvent occupancy noted to date at 45.7%).[8] This lower volume is reflected in the larger density of **1** (1.519 $g\,cm^{-3}$) compared to those of previously reported structures [e.g. 1.485 $g\,cm^{-3}$ for the dinickel(II) compound].[8]

Thermal Analysis of 1

Thermogravimetric analysis (TGA) was performed on powdered samples of **1**. The sample was ramped from ca. 25 to 500 °C at a rate of 10 °C/min under nitrogen. The TGA curve of **1** is shown in Figure 3. The slight inflection at ca. 90 °C after a mass loss of 5.6% is indicative of the

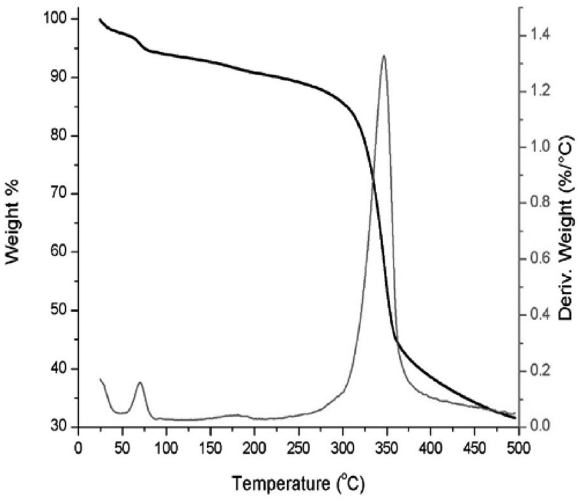

Figure 3. TGA curve of **1** indicating initial loss of solvent and decomposition of the dimeric species at ca. 300 °C.

loss of free methanol molecules. Decomposition of the dinuclear species at ca. 300 °C is consistent with the loss of the phen ligands.

Magnetic Behavior of 1

The magnetic properties of complex **1** in the form of both $\chi_M T$ and χ_M vs. T plots [χ_M is the magnetic susceptibility per two cobalt(II) ions] are shown in Figure 4. At room temperature, $\chi_M T$ is equal to 6.0 $cm^3 mol^{-1} K$. This value remains practically constant upon cooling to 100 K, and then it decreases sharply to 1.13 $cm^3 mol^{-1} K$ at 1.9 K. The μ_{eff} value per Co^{II} ion at room temperature is equal to 4.90 μ_B, a value which is larger than expected for the spin-only case (μ_{eff} = 3.87 μ_B, S = 3/2). This indicates that an important orbital contribution occurs in **1**, which is responsible for the decrease of $\chi_M T$ below 100 K. In fact, six-coordinate high-spin Co^{II} ions have a $^4T_{1g}$ triplet ground state and the distortion of the octahedral symmetry of the cobalt atoms in **1** is not significant enough to induce total quenching of the orbital momentum of the low-lying $^4T_{1g}$ state. The presence of a maximum in the susceptibility plot at 3.0 K indicates the occurrence of a weak but significant antiferromagnetic interaction between the paramagnetic centers in **1**.

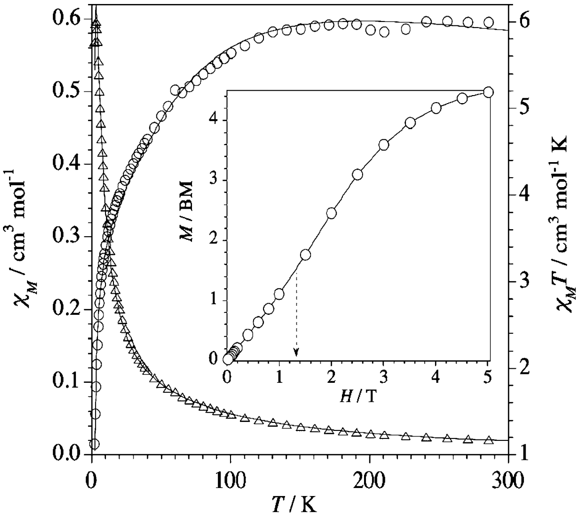

Figure 4. Thermal dependence of χ_M (triangles) and $\chi_M T$ (circles) for **1**. The solid line is the best-fit curve for a cobalt(II) dimer with J and g as variable parameters (see text). The inset shows the magnetization versus H plot of **1** at 2.0 K.

In general, the spin Hamiltonian is insufficient to treat the magnetic properties of six-coordinate cobalt(II) complexes because of the important first-order orbital momentum that this cation exhibits. Thus, the Hamiltonian has to be supplemented by the consideration of orbitally dependent exchange interactions as well as spin–orbit coupling effects.[14] We have recently shown that the magnetic properties of six-coordinate dinuclear cobalt(II) complexes can be appropriately described by using a Hamiltonian that includes four terms [Equation (1)]: (a) the magnetic exchange coupling between the two spins quartets ($S_1 = S_2 = 3/2$) of the Co^{II} ions, (b) the spin-orbit coupling of the $^4T_1$ ground term in octahedral symmetry, (c) the splitting of the T_1 orbital term in a singlet and a doublet orbital terms (Δ being the energy gap) due to an axial symmetry, and (d) the Zeeman interaction.[15]

$$\hat{\mathrm{H}} = -J\hat{S}_1\hat{S}_2 - \sum_{i=1}^{2}\alpha\lambda\hat{L}_i\hat{S}_i + \sum_{i=1}^{2}\Delta[\hat{L}_{zi}^2 - 2/3] + \beta H\sum_{i=1}^{2}(-\alpha\hat{L}_i + g_e\hat{S}_i) \tag{1}$$

λ is the spin-orbit coupling parameter, α is an orbital reduction factor defined as $\alpha = Ak$ where k considers the reduction of the orbital momentum caused by the delocalization of the unpaired electrons, and A is a crystal-field parameter (A = 1.5 and 1 for the weak and strong crystal-field limits, respectively). In the frame of T_1 and P term isomorphism, $\boldsymbol{L}(T_{1g}) = -A\boldsymbol{L}(P)$, we can use L = 1 and treat the term $\alpha\lambda\hat{L}\hat{S}$ as an isotropic Hamiltonian describing the interaction between the two angular momenta L = 1 and S = 3/2, $\alpha\lambda$ being the coupling parameter, and $\Delta[L^2_z - 2/3]$ as a zero-field splitting of the angular momentum L = 1. Least-squares fit of the magnetic susceptibility data of **1** gave $\lambda = -110\ cm^{-1}$, α = 1.32 (for instance, k = 0.91 with A = 1.45), $\Delta = -390\ cm^{-1}$, and $J = -1.23\ cm^{-1}$. The calculated curve matches well the magnetic data over the whole temperature range (solid line in Figure 4).

The M vs. H plot (M being the magnetization per Co^{II} ions) at 2.0 K for **1** (see inset of Figure 4) provides additional support for both the nature and magnitude of the magnetic coupling between the paramagnetic centers. This curve exhibits an inflection point at ca. 1.3 T, which is interpreted as the overcoming of the antiferromagnetic coupling by the applied magnetic field, the energy involved being ca. 1.3 cm^{-1} (estimated value as $g\beta H$ with g = 2.0). The value of the saturation magnetization is ca. 4.40 μ_B, which is in agreement with the calculated value for two Co^{II} ions with an effective spin S'_{Co} = 1/2 and a value of g_{Co} = 4.21 given by $g_{Co} = (10 + 2\alpha)/3$ ($M_s = 2g_{Co}S'_{Co}$ = 4.21 μ_B). In fact, only the ground Kramer's doublet of each Co^{II} ion is populated at 2.0 K.

The value of the antiferromagnetic coupling through the bridging pyrophosphato ligand in **1** lies in the range of the previous values observed in only very few related dinuclear species with other first-row transition-metal ions (see Table 3). The exchange pathway is easily visualized with the dicopper(II) complex where each metal ion has only one unpaired electron (so-called magnetic orbital) which is described by a $d_{x^2-y^2}$ orbital [with x- and y-axes being roughly described by the Cu–N(bipy) bonds]. The poor overlap between these two magnetic orbitals through the two nonlinear O–P–O bridging motifs [the Cu–(μ-pyrophosphato)–Cu has a "roof" shape] accounts for the weak antiferromagnetic coupling. The number of unpaired electrons increases from one in Cu^{II}, two in Ni^{II}, three in Co^{II} up to five in Mn^{II}, with additional σ- and π-pathways becoming operative. The magnitude of the antiferromagnetic interaction is then properly described not by J, but by $n_A n_B J$.[16] As the energy of the 3d orbitals decreases when going from Mn^{II} to Cu^{II}, the energy gap between these orbitals and that of

Table 3. Selected magneto-structural data for pyrophosphato-bridged dinuclear metal complexes.

Compound	M–O(pyro.)[a] [Å]	$d_{M–M}$[b] [Å]	–J[c] [cm^{-1}]	n_An_BJ[d] [cm^{-1}]	Ref.
$\{[Cu(bipy)(H_2O)]_2(\mu\text{-}P_2O_7)\}$ $7H_2O$	1.950	4.646	20	20	[10]
$\{[Ni(phen)_2]_2(\mu\text{-}P_2O_7)\}$ $27H_2O$	2.057	5.031	3.8	15.2	[8]
$\{[Co(phen)_2]_2(\mu\text{-}P_2O_7)\}\cdot 6MeOH$	2.043	4.857	1.23	11.1	this work
$\{[Mn(phen)_2]_2(\mu\text{-}P_2O_7)\}\cdot 13H_2O$	2.105	4.700	0.88	22.0	[8]

[a] Average value for the metal–oxygen (bridging pyrophosphato ligand) bond. [b] Metal–metal separation across the pyrophosphato ligand. [c] Exchange interaction through the bridging pyrophosphato ligand. [d] n_A and n_B are the numbers of the unpaired electrons on the metal atoms A and B of the AB dinuclear complex.

the symmetry-adapted HOMOs of the bridging pyrophosphato ligand becomes smaller when going from Mn^{II} to Cu^{II} compounds. This would induce a better overlap between the magnetic orbitals when going from Mn^{II} to Cu^{II} and then an increasing antiferromagnetic interaction along these series. This is what is observed for the Co^{II}, Ni^{II} and Cu^{II} pyrophosphate series, the antiferromagnetic coupling in the case of the Mn^{II} being too large. Most likely, the origin of this apparent discrepancy lies on subtle structural differences. In fact, the intramolecular metal–metal separation in the manganese compound is nearly equal to that of the copper(II) compound and significantly smaller than those of the corresponding cobalt(II) and nickel(II) complexes. The greater distortion of the manganese N_4O_2 chromophore could cause a strengthening of the overlap between the interacting magnetic orbitals and thus a greater antiferromagnetic coupling.

We would like to finish this contribution with a brief comparison between the ability of the pyrophosphato and oxalato (ox) ligands to mediate magnetic interactions when adopting the bis(bidentate) coordination mode in its metal complexes. Let us focus on the copper(II) complexes where the magnetic interactions are expected to be larger. In fact, the largest antiferromagnetic coupling for oxalato-bridged copper(II) complexes is J = –386 cm^{-1}, and this strong interaction is observed for planar Cu^{II}–(μ-ox)–Cu^{II} units with the Cu–O(ox) bonds in the equatorial plane.[17] The good σ in-plane overlap between the two coplanar magnetic orbitals accounts for this strong antiferromagnetic coupling whose dependence of subtle structural and electronic factors has been subject of a great number of experimental and theoretical works.[17–19] The planarity of the Cu–O–C–O–Cu skeleton is lost in the Cu–O–P–O–Cu pathway due to the sp^3 hybridization of the phosphorus atom of the pyrophosphate moiety. Consequently, the Cu–(μ-pyrophosphato)–Cu exhibits a roof shape, and the overlap between the two $d_{x^2-y^2}$ magnetic orbitals is decreased leading to a much weaker antiferromagnetic coupling [J = –20 cm^{-1} for $\{[Cu(bipy)(H_2O)_2]_2(\mu\text{-}P_2O_7)\}\cdot 7H_2O$ vs. J = –380 cm^{-1} for $\{[Cu(bipy)(H_2O)]_2(\mu\text{-}ox)\}(NO_3)_2\cdot[Cu(bipy)(ox)]$.[10,17]

Conclusions

We have successfully synthesized a pyrophosphato-bridged cobalt(II) coordination complex and conducted a full magnetic characterization. This complex is critical in our attempt to better understand the relationship between structure and function in pyrophosphato-bridged species. We have been able, using this cobalt system and that of complexes previously reported, to explain and rationalize the significant coupling facilitated by the pyrophosphate group and reasoned the comparative weakness of the coupling, compared to oxalate. This weakness is due in part, to distortions in the structure due to phosphorus sp^3 hybridization resulting in decreased overlap in key magnetic orbitals. This is to the best of our knowledge the first such in-depth structure–function study/comparison of pyrophosphato-bridged complexes. An understanding of structure–function relationships allows us to predict the possibility of producing a ferromagnetic system bridged by the pyrophosphato ligand. A series of compounds based on such predictions are currently being prepared for structural and magnetic characterization. In addition, the magnetic interaction of metal atoms in proteins and enzymes has long been of interest to biologists and chemists. Given the importance of pyrophosphate and its interactions with metal ions in biology, especially in regard to enzymes such as the manganese- and magnesium-containing PPases, which bind the pyrophosphate substrate such that hydrolysis by nucleophilic attack of metal-bound water can take place, an intricate understanding of effects of exchange interactions between metal centers can only lead to a greater understanding of such a unique family of proteins.[23]

Experimental Section

General: Solvents and chemicals were of laboratory grade and were used as received. Electrospray mass spectrometry was performed with a Shimadzu LCMS-2010 A system at a cone voltage of 5 kV. IR spectra were recorded with a Nicolet Magna-IR 850 Series II spectrophotometer as KBr pellets. Thermal analysis was performed with a TA instruments TGA Q500 using 2–6 mg samples placed on platinum pans and run under nitrogen (40 mL/min). The temperature was ramped from ca. 25 to 500 °C at a rate of 10 °C/min. Analysis was performed using the TA instruments Universal Analysis 2000 software program. Elemental analysis (C, H, N) was performed by Atlantic Microlab, Inc., Norcross, GA and Complete Analysis Laboratories, Inc., Parsippany, NY. Water was distilled and deionized to 18.6 MΩ using a Barnstead Diamond RO Reverse Osmosis machine coupled to a Barnstead Nano Diamond ultrapurification machine. Variable-temperature magnetic susceptibility measurements were performed with a Quantum design SQUID susceptometer in the temperature range 1.9–295 K with an applied magnetic field of H = 10000 G ($T \geq 50$ K) and 500 G ($T < 50$ K). Crystalline samples were obtained directly from the reaction mixture, air-dried and powdered in a mortar. Diamagnetic corrections for the constituent atoms were estimated using Pascal's constants, and corrections for the sample holder were also performed. Electronic absorption spectra were obtained with a Varian Cary 50 Bio spectrophotometer in 1 mL Quartz cuvettes between 200 and 800 nm at ambient temperature.

Synthesis and Characterization of $\{[Co(phen)_2]_2(\mu\text{-}P_2O_7)\cdot 6MeOH\}$ (1): Cobalt(II) sulfate heptahydrate (0.29 g, 1.0 mmol) was dissolved in 15 mL of water. To this was added an aqueous suspension of 1,10-phenanthroline (0.36 g, 2.2 mmol) resulting in an orange solution. Solid sodium pyrophosphate (0.13 g, 0.49 mmol) was added directly, and a peach-colored precipitate was observed after 2 min. The solid was dissolved in a minimum amount of methanol and filtered (0.45 μM Fisher). Crystallization was conducted by a methanol/petroleum ether diffusion performed under ambient conditions. Red block crystals formed over ca. 6 d. $C_{54}H_{56}Co_2N_8O_{13}P_2$ (1204.87): calcd. C 53.9, H 4.70, N 9.30; found C 53.5, H 4.72, N 9.28. UV/Vis (MeOH): λ_{max} (ε) = 226 (28383 M^{-1} cm^{-1}) nm. FTIR (KBr): $\tilde{\nu}$ = 1625 (w), 1516 (s), 1497 (s), 1424 (s), 1342 (s), 1180 (sh), 1103 (br), 1021 (s), 906 (m), 849 (s), 725 (s), 566 (w) cm^{-1}. ESMS (MeOH/0.1%TFA): m/z = 507.1 $[Co(phen)_2]_2(\mu\text{-}P_2O_7)\text{-}2H^+]^{2+}$.

Crystal Determination and Refinement of the Structure: Structural measurements were performed with a Bruker-AXS SMART-CCD diffractometer at low temperature (90 K) using graphite-monochromated Mo-K_α radiation (λ = 0.71073 Å). Absorption corrections were applied using SADABS[20] and SHELXTL.[21] The structure was solved by direct methods and refined using the SHELXTL[22] program package. Key crystallographic data are given in Table 4. CCDC-675348 contains the supplementary crystallographic data for this paper. These data can be obtained free of charge from The Cambridge Crystallographic Data Centre via www.ccdc.cam.ac.uk/data_request/cif.

Table 4. Crystallographic details for **1**.

	1
Empirical formula	$C_{54}H_{56}Co_2N_8O_{13}P_2$
Formula mass	1204.87
Crystal system	triclinic
Space group	$P\bar{1}$
λ(Mo-K_α) [mm^{-1}]	0.765
a [Å]	12.6948(11)
b [Å]	13.2729(11)
c [Å]	16.1807(14)
α [°]	85.788(2)
β [°]	86.875(2)
γ [°]	75.875(2)
V [Å^3]	2634.9(4)
Z	2
D_c [$g\,cm^{-3}$]	1.519
θ_{max}	28.08
R, wR_2 [$I > 2\sigma(I)$]	0.0369, 0.0961
R, wR_2 (all data)	0.0434, 0.1005
Reflections:	
collected	27668
observed	12755

Acknowledgments

We thank the Syracuse University (iLEARN program) and the Ministerio Español de Educación y Ciencia (Project CTQ2007-61690) for funding.

[1] J. Wang, G. S. Sheppard, P. Lou, M. Kawai, C. Park, D. A. Egan, A. Schneider, J. Bouska, R. Lesniewski, J. Henkin, *BioChem* **2003**, *42*, 5035–5042.

[2] J. H. Martens, H. Barg, M. J. Warren, D. Jahn, *Appl. Microbiol. Biotechnol.* **2002**, *58*, 275–285.

[3] R. P. Doyle, M. Nieuwenhuyzen, P. E. Kruger, *Dalton Trans.* **2005**, 3745–3750.

[4] a) D. E. Wilcox, *Chem. Rev.* **1996**, *96*, 2435–2458; b) A. A. Baykov, B. S. Copperman, A. Goldman, R. Lahti, *Prog. Mol. Subcell. Biol.* **1999**, *23*, 127–150.

[5] H. Harutyunyan, I. P. Kuranova, B. K. Vainshtein, W. E. Hohne, V. S. Lamzin, Z. Dauter, A. V. Teplyakov, K. S. Wilson, *Eur. J. Biochem.* **1996**, *239*, 220–228.

[6] a) P. Heikinheimo, V. Tuominen, A. K. Ahonoe, A. Teplyakov, B. S. Cooperman, A. A. Baykov, R. Lahti, A. Goldman, *Proc. Natl. Acad. Sci. USA* **2001**, *98*, 3121–3126; b) A. B. Zyryanov, A. S. Shetakov, R. Lahiti, A. A. Baykov, *Biochem. J.* **2002**, *367*, 901–906.

[7] a) T. Kasuga, M. Terada, M. Nogamin, M. Niinomi, *J. Mater. Res.* **2001**, *16*, 876–880; b) S. T. Wilson, B. M. Lok, C. A. Messian, T. R. Cannon, E. M. Flanigen, *J. Am. Chem. Soc.* **1982**, *104*, 1146–1147; c) X. Sun, X. G. Xu, Y. J. Fu, S. L. Wang, H. Zeng, Y. P. Li, *Cryst. Res. Technol.* **2001**, *4–5*, 465–470.

[8] O. F. Ikotun, N. G. Armatus, M. Julve, P. E. Kruger, F. Lloret, M. Nieuwenhuyzen, R. P. Doyle, *Inorg. Chem.* **2007**, *46*, 6668–6674.

[9] E. W. Ainscough, A. M. Brodie, J. D. Ranford, J. M. Waters, K. S. Murray, *Inorg. Chim. Acta* **1992**, *197*, 107–115.

[10] P. E. Kruger, R. P. Doyle, M. Julve, F. Lloret, M. Niewenhuyzen, *Inorg. Chem.* **2001**, *40*, 1726–1727.

[11] J. Y. Xu, J. L. Tian, Q. W. Zhang, J. Zhao, S. P. Yan, D. Z. Liao, *Inorg. Chem. Commun.* **2008**, *11*, 69–72.

[12] Y. Funahashi, A. Yoneda, C. Taki, M. Kosuge, T. Ozawa, K. Jitsukawa, H. Masuda, *Chem. Lett.* **2005**, *34*, 1332–1333.

[13] N. Heron, D. L. Thorn, R. L. Harlow, G. W. Coulston, *J. Am. Chem. Soc.* **1997**, *119*, 7149–7150.

[14] K. Nakamoto, *Infrared and Raman Spectra of Inorganic and Coordination Compounds*, Part B (Applications in Coordination, Organometallics and Bioinorganic Chemistry), 5th ed., Wiley, Chichester, **1997**.

[15] a) V. Mishra, F. Lloret, R. Mukherjee, *Inorg. Chim. Acta* **2006**, *359*, 4053; b) D. Maspoch, N. Domingo, D. Ruiz-Molina, K. Wurst, J. M. Hernández, F. Lloret, J. Tejada, C. Rovira, J. Veciana, *Inorg. Chem.* **2007**, *46*, 1627; c) A. K. Sharma, F. Lloret, R. Mukherjee, *Inorg. Chem.* **2007**, *46*, 5128; d) J. M. Herrera, A. Bleuzen, Y. Dromzée, M. Julve, F. Lloret, M. Verdaguer, *Inorg. Chem.* **2003**, *42*, 7052; e) O. Fabelo, J. Pasán, F. Lloret, M. Julve, C. Ruiz-Pérez, *CrystEngComm* **2007**, *9*, 815; f) D. Maspoch, N. Domingo, D. Ruiz-Molina, K. Wurst, J. M. Hernandez, G. Vaughan, C. Rovira, F. Lloret, J. Tejada, J. Veciana, *Chem. Commun.* **2005**, 5035; g) A. Rodríguez, H. Sakiyama, N. Masciocchi, S. Galli, N. Gálvez, F. Lloret, E. Colacio, *Inorg. Chem.* **2005**, *44*, 8399; h) L. Cañadillas-Delgado, O. Fabelo, J. Pasán, F. S. Delgado, F. Lloret, M. Julve, C. Ruiz-Pérez, *Inorg. Chem.* **2007**, *46*, 7458; i) G. De Munno, T. Poerio, M. Julve, F. Lloret, G. Viau, *New J. Chem.* **1998**, 299; j) G. De Munno, M. Julve, F. Lloret, J. Faus, A. Caneschi, *J. Chem. Soc., Dalton Trans.* **1994**, 1175.

[16] O. Kahn, *Struct. Bonding (Berlin, Ger.)* **1987**, *68*, 89 and references cited therein.

[17] a) M. Julve, J. Faus, M. Verdaguer, A. Gleizes, *J. Am. Chem. Soc.* **1984**, *106*, 8306–8308; b) A. Gleizes, M. Julve, M. Verdaguer, J. A. Real, J. Faus, X. Solans, *J. Chem. Soc., Dalton Trans.* **1992**, 3209–3216.

[18] a) T. R. Felthouse, E. J. Laskowski, D. N. Hendrickson, *Inorg. Chem.* **1977**, *16*, 1077–1089; b) M. Julve, M. Verdaguer, O. Kahn, A. Gleizes, M. Philoche-Levisalles, *Inorg. Chem.* **1983**, *22*, 368–370; c) M. Julve, M. Verdaguer, A. Gleizes, M. Philoche-Levisalles, O. Kahn, *Inorg. Chem.* **1984**, *23*, 3808–3818; d)

L. Soto, J. García, E. Escrivá, J.-P. Legros, J.-P. Tuchgues, F. Dahan, A. Fuertes, *Inorg. Chem.* **1989**, *28*, 3378–3386; e) J. Glerup, P. A. Goodson, D. J. Hodgson, K. Michelsen, *Inorg. Chem.* **1995**, *34*, 6255–6264; f) P. Román, C. Guzmán-Miralles, A. Luque, J. I. Beitia, J. Cano, F. Lloret, M. Julve, S. Alvarez, *Inorg. Chem.* **1996**, *35*, 3741–3751; g) O. Castillo, A. Luque, P. Román, F. Lloret, M. Julve, *Inorg. Chem.* **2001**, *40*, 5526–5535.

[19] a) S. Alvarez, M. Julve, M. Verdaguer, *Inorg. Chem.* **1990**, *29*, 4500–4507; b) J. Cano, P. Alemany, S. Alvarez, M. Verdaguer, E. Ruiz, *Chem. Eur. J.* **1998**, *4*, 476–484.

[20] A. L. Speck, *PLATON*, *A Multipurpose Crystallographic Tool*, Utrecht University, Utrecht, The Netherlands, **2000**; *Mercury 1.1*, CCDC, Cambridge, **2002**.

[21] G. M. Sheldrick, *SHELXTL, A System for Structure Solution and Refinement*, version 5.0, Bruker-AXS, Madision, WI, **1998**.

[22] *SHELXTL PC*, version 6.1, Bruker-AXS, Inc., Madision, WI, **2002**.

[23] J. Kankare, T. Salminen, R. Lahti, B. S. Cooperman, A. A. Baykov, A. Goldman, *Biochemistry* **1996**, *35*, 4670–4677.

Received: February 22, 2008